

Distribution of Dust around Galaxies: An Analytic Model

Shogo Masaki^{1*†} and Naoki Yoshida^{2,3}

¹*Department of Physics, Nagoya University, Chikusa, Nagoya 464-8602, Japan*

²*Kavli Institute for the Physics and Mathematics of the Universe, TODIAS, University of Tokyo, Kashiwa 277-8583, Japan*

³*Department of Physics, University of Tokyo, Tokyo 113-0033, Japan*

Accepted . Received ; in original form

ABSTRACT

We develop an analytic halo model for the distribution of dust around galaxies. The model results are compared with the observed surface dust density profile measured through reddening of background quasars in the Sloan Digital Sky Survey (SDSS) reported by Ménard et al. (2010a). We assume that the dust distribution around a galaxy is described by a simple power law, similarly to the mass distribution, but with a sharp cut-off at αR_{vir} where R_{vir} is the galaxy's virial radius and α is a model parameter. Our model reproduces the observed dust distribution profile very well over a wide range of radial distance of $10 - 10^4 h^{-1} \text{kpc}$. For the characteristic galaxy halo mass of $2 \times 10^{12} h^{-1} M_{\odot}$ estimated for the SDSS galaxies, the best fit model is obtained if α is greater than unity, which suggests that dust is distributed to over a few hundred kilo-parsecs from the galaxies. The observed large-scale dust distribution profile is reproduced if we assume the total amount of dust is equal to that estimated from the integrated stellar evolution over the cosmic time.

Key words: large scale structure of Universe - galaxies: haloes - intergalactic medium

1 INTRODUCTION

How matter is distributed around galaxies is one of the fundamental questions in cosmology. Gravitational lensing provides a powerful method to map the matter distribution at small and large length scales (for a review, see Bartelmann & Schneider 2001). Recent large galaxy redshift surveys, such as the Sloan Digital Sky Survey (SDSS; York et al. 2000) and COSMOS survey, have allowed us to explore the mean surface density profile of galaxies through weak lensing techniques (e.g., Sheldon et al. 2004; Mandelbaum et al. 2006; Ménard et al. 2010a; Leauthaud et al. 2012).

Ménard et al. (2010a, hereafter MSFR) measured the mean surface matter density profile of the SDSS main galaxies with the mean redshift $\langle z \rangle = 0.36$ through gravitational lensing magnification of background quasars (QSOs). They calculated the cross-correlation between the number density of foreground galaxies and the flux magnification of background QSOs. The cross-correlation function was then converted to the surface matter density profile Σ_m of the lens galaxies as a function of the projected distance R from the galactic center. The derived profile is well approximated as $\Sigma_m \propto R^{-0.8}$ at $10 \text{kpc} \lesssim R \lesssim 10 \text{Mpc}$.

MSFR also detected the systematic offset between the

five SDSS photometric bands in magnification of background QSOs; in shorter wavelength, QSOs appear less magnified. It is interpreted as reddening due to dust in and around foreground galaxies. Adopting the small Magellanic cloud type dust model for the sample galaxies, they derived the mean surface dust density profile of galaxies $\Sigma_d(R)$ from the galaxy-QSO color cross-correlation function. The shape of the derived Σ_d is very similar to that of Σ_m at $10 \text{kpc} \lesssim R \lesssim 10 \text{Mpc}$, suggesting that there is a substantial amount of dust in the galactic halos (see also Chelouche et al. 2007; McGee & Balogh 2010). Theoretical models are needed to properly interpret the observationally inferred dust distribution.

In this Letter, we develop an analytic model based on the so-called halo approach to study the distribution of dust around galaxies. Earlier in Masaki, Fukugita & Yoshida (2012), we used cosmological N -body simulations to study in detail the matter distribution around galaxies. There, we showed that the observed surface density profile can be used to determine the characteristic mass of the sample lens galaxies, and that the mass distributed beyond the galaxies' virial radii contributes about half of the global mass density. We provide a physical model for the dust distribution in this Letter. Our model is characterized by two key physical parameters; one is the host halo mass of the galaxies and the other is the extent of dust distribution. The former is determined from the observed matter profile (e.g., Mandelbaum et al. 2006; Hayashi & White 2008; Leauthaud et al. 2012; Masaki, Fukugita & Yoshida 2012),

* E-mail: shogo.masaki@nagoya-u.jp

† JSPS Fellow

while the latter can be inferred from the dust distribution. How far dust is transported from the galaxies is indeed a highly interesting question. The observed dust profile is well described by a single power law over a wide range of distance of from 10kpc to 10Mpc. We show that the profile is decomposed into two parts, the so-called one-halo and two-halo terms. We parametrize the one-halo term such that dust is distributed to αR_{vir} where R_{vir} is the galaxy's virial radius. Through model fitting, we determine the extension parameter α to be greater than unity. We discuss the implication for the dust production and transport mechanism into intergalactic space.

2 THE MODEL

2.1 Halo approach

We present a simple formulation to calculate the surface dust density profile. Our model is based on the so-called halo approach (Seljak 2000; Cooray & Sheth 2002). The mean surface density $\Sigma_d(R)$ is divided into two terms:

$$\Sigma_d(R) = \Sigma_d^{\text{1h}}(R) + \Sigma_d^{\text{2h}}(R), \quad (1)$$

where R is the distance in the projected two-dimensional plane. The one-halo term $\Sigma_d^{\text{1h}}(R)$ arises from the central halo, and the two-halo term $\Sigma_d^{\text{2h}}(R)$ from the neighbouring halos.

The contribution from an individual galaxy halo with mass M_h to the one-halo term $\Sigma_d^{\text{1h}}(R)$ is given by the projection of the halo dust density profile $\rho_d(r|M_h)$ along the line-of-sight χ :

$$\Sigma_d(R|M_h) = \int_{-\infty}^{\infty} d\chi \rho_d(r = \sqrt{\chi^2 + R^2} | M_h). \quad (2)$$

The one-halo term is then a number-weighted average of $\Sigma_d(R|M_h)$

$$\Sigma_d^{\text{1h}}(R) = \frac{1}{n_{\text{halo}}} \int_{M_{\text{min}}}^{\infty} dM_h \frac{dn}{dM_h} \Sigma_d(R|M_h), \quad (3)$$

$$n_{\text{halo}} = \int_{M_{\text{min}}}^{\infty} dM_h \frac{dn}{dM_h}, \quad (4)$$

where dn/dM_h is the halo mass function and M_{min} is the threshold halo mass for the sample galaxies. The threshold mass corresponds to the typical host halo mass of the observed galaxies.

We calculate the two-halo term power spectrum $P_d^{\text{2h}}(k)$ as follows:

$$\begin{aligned} P_d^{\text{2h}}(k) &= P_{\text{lin}}(k) \\ &\times \left[\frac{1}{\bar{\rho}_d} \int_0^{\infty} dM_h \frac{dn}{dM_h} M_d(M_h) b(M_h) u_d(k|M_h) \right] \\ &\times \left[\frac{1}{n_{\text{halo}}} \int_{M_{\text{min}}}^{\infty} dM_h \frac{dn}{dM_h} b(M_h) u_d(k|M_h) \right], \quad (5) \end{aligned}$$

where $\bar{\rho}_d$ is the mean cosmic dust density, $P_{\text{lin}}(k)$ is the linear matter power spectrum, $b(M_h)$ is the halo bias factor, $M_d(M_h)$ is dust mass in and around a halo with mass M_h , and $u_d(k|M_h)$ is the Fourier transform of the density profile ρ_d normalized by its dust mass. The power spectrum is converted to the two-point correlation function via

$$\xi_d^{\text{2h}}(r) = \frac{1}{2\pi^2} \int_0^{\infty} dk k^2 \frac{\sin(kr)}{kr} P_d^{\text{2h}}(k). \quad (6)$$

Then we obtain the two-halo term of the mean surface density profile

$$\begin{aligned} \Sigma_d^{\text{2h}}(R) &= \bar{\rho}_d \int_{-\infty}^{\infty} d\chi \xi_d^{\text{2h}}(r = \sqrt{\chi^2 + R^2}) \\ &= 2\bar{\rho}_d \int_R^{\infty} dr \frac{r \xi_d^{\text{2h}}}{\sqrt{r^2 - R^2}}. \quad (7) \end{aligned}$$

We adopt a flat- Λ CDM cosmology, with $\Omega_m = 0.272$, $\Omega_\Lambda = 0.728$, $H_0 = 70.2 \text{ km s}^{-1} \text{ Mpc}^{-1}$, $n_s = 0.961$ (Komatsu et al. 2011). We use the code *CAMB* to obtain the linear matter powerspectrum (Lewis, Challinor & Lasenby 2000) and utilize the halo mass function and bias given by Sheth & Tormen (1999) at $z = 0.36$ which is equal to the mean redshift of the galaxy sample used in MSFR.

2.2 Dust distribution profile

We assume that the spatial distribution of dust within and around a halo is organized as

$$\rho_d(r|M_h) \propto \frac{1}{r^2} \exp\left(-\frac{r}{\alpha R_{\text{vir}}}\right). \quad (8)$$

where R_{vir} is the virial radius. Within the virial radius R_{vir} , the mean internal matter density is $\Delta \times \rho_{\text{crit}}$, where Δ is given by Bryan & Norman (1998). Essentially, we assume that the dust distribution follows a singular isothermal sphere (SIS) profile with exponential cut-off at $r = \alpha R_{\text{vir}}$. One of our aims in this Letter is to determine the value of α , i.e., how far dust is distributed from galaxies. Fig. 1 shows the shape of the dust density profile ρ_d for a halo with mass $M_h = 10^{13} h^{-1} M_\odot$ computed in the above manner. We see the dependence on α clearly.

The power-law shape is motivated by the fact that the observationally derived surface dust profile itself is well fit by a simple power law of $\Sigma_d \propto R^{-0.8}$, similarly to matter distribution (MSFR). Also, detailed calculations of dust ejection and radiation-driven transport by Bianchi & Ferrara (2005) show approximately a power-law distribution for the resulting gas metallicity through dust sputtering. We have also examined other profiles of the form r^{-3} and r^{-1} with a similar exponential cut-off. However, we have found that neither of the steeper or the shallower profile reproduces well the observed dust profile at small distances. We therefore adopt the profile equation (8) in our model.

The Fourier transform of $\rho_d(r)$ is given by

$$u_d(k|M_h) = \int_0^{\infty} dr 4\pi r^2 \frac{\sin(kr)}{kr} \frac{\rho_d(r|M_h)}{M_d(M_h)}. \quad (9)$$

Note that the value of u_d should be unity in small- k limit. We determine the amplitude of ρ_d by setting the halo dust mass associated with a halo to be a certain value M_d . To this end, we first consider the total amount of dust around galaxies in the local universe. Fukugita (2011) estimated the total amount, in units of the cosmic density parameter,

$$\Omega_{\text{galaxy dust}} = 4.7 \times 10^{-6}. \quad (10)$$

Interestingly, this value is close to the difference between the estimated amount of dust produced and shed by stars over

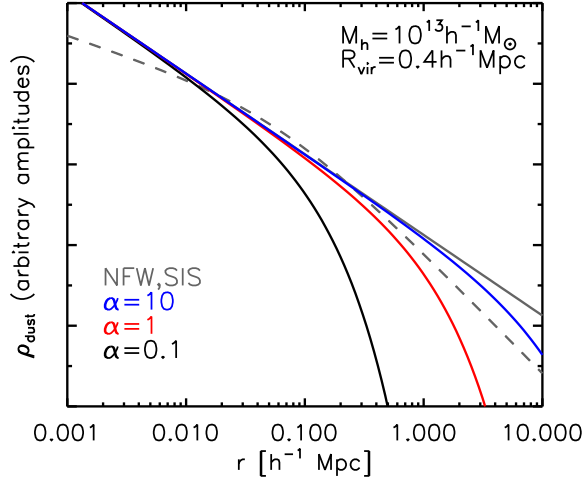


Figure 1. The model dust density profile as a function of the spatial distance from the center. The black, red and blue lines represent the model profiles with $\alpha = 0.1, 1$ and 10 , respectively. For comparison, we also show the NFW (Navarro et al. 1997) and the untruncated SIS profiles by grey lines. Note that the amplitudes are arbitrary in this figure.

the age of the universe and the summed amount found in local galactic discs (see also Inoue & Kamaya 2003). Suppose that the comoving density of the total halo dust remains constant in the local universe. Then the mean cosmic density of dust in galactic halos is given by

$$\bar{\rho}_d(z) = \Omega_{\text{galaxy dust}} \rho_{\text{crit}}(z)(1+z)^3. \quad (11)$$

We set the dust mass associated with a halo to be

$$\int_0^\infty dr 4\pi r^2 \rho_d(r|M_h) = M_d = \Gamma \times M_h \quad (12)$$

where Γ is the dust-halo mass ratio. We integrate the dust mass weighted by the halo mass function to obtain the global dust density. We normalize ρ_d , or equivalently Γ , by matching the global dust density to equation (11). Note that Γ is not necessarily a constant but can be a function of halo mass.

2.2.1 Dust-halo mass ratio Γ

An essential physical quantity in our model is the dust-halo mass ratio Γ in equation (12). We propose two simple models. The first one is *constant model*, i.e., Γ is independent of halo mass. The dust-halo mass ratio is simply the global density ratio

$$\Gamma = 1.73 \times 10^{-5} = \Omega_{\text{galaxy dust}} / \Omega_m. \quad (13)$$

Because the heavy elements that constitute dust are produced by stars, it may be reasonable to expect that the dust mass is proportional to the stellar mass. Intriguingly, Takeuchi et al. (2010) used data of AKARI and GALEX to show a moderate correlation between the stellar mass and dust attenuation indicator for the sample galaxies (see their Figure 16). In our second model, we consider the observed galaxy stellar-halo mass relation to model the halo mass dependence of Γ . We call the model as *mass dependent*

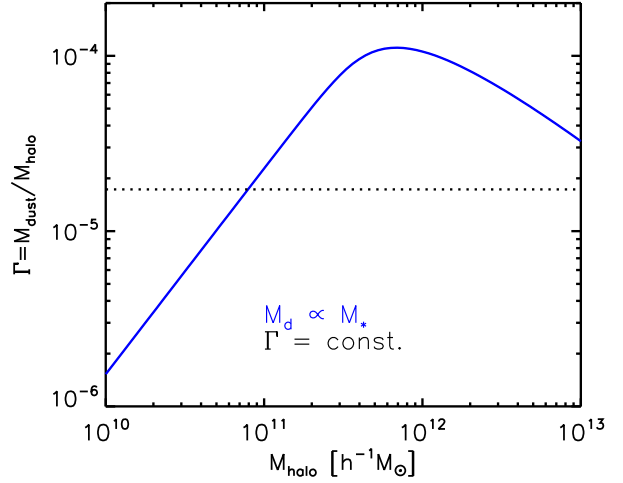


Figure 2. Two models for dust-halo mass ratio as a function of halo mass. The dashed and the solid lines are the ratio Γ for the constant and the mass dependent model, respectively.

model. Leauthaud et al. (2012) recently studied the stellar-halo mass relation from the joint analysis of galaxy-galaxy weak lensing, galaxy clustering and galaxy number densities using the COSMOS survey data. We use their functional form with the best fit parameters at $z \approx 0.37$,

$$\begin{aligned} \log_{10}(M_h) &= \log_{10}(M_1) + \beta \log_{10} \left(\frac{M_*}{M_{*,0}} \right) \\ &+ \frac{(M_*/M_{*,0})^\delta}{1 + (M_*/M_{*,0})^{-\gamma}} - 0.5, \end{aligned} \quad (14)$$

where M_* is the galaxy stellar mass, $\log_{10}(M_1/M_\odot) = 12.52$, $\log_{10}(M_{*,0}/M_\odot) = 10.92$, $\beta = 0.46$, $\delta = 0.57$, and $\gamma = 1.5$ (see also Behroozi, Conroy, & Wechsler 2010). We then relate the dust mass to the stellar mass as

$$M_d(M_h) \propto M_*(M_h). \quad (15)$$

The normalization constant is determined to be 3.05×10^{-3} by integrating this equation weighted by the halo mass function. The global dust mass density thus calculated is matched to equation (11).

Fig. 2 compares Γ for our two models. The shape of Γ for the mass-dependent model reflects the stellar-halo mass relation. The peak value of Γ at $\sim 6 \times 10^{11} h^{-1} M_\odot$ is $\simeq 10^{-4}$. Overall, Γ for the mass dependent model is larger than that for the constant model at the characteristic mass of the sample galaxies (see Section 3).

We are now able to calculate the dust surface density profile. In Fig. 3, we show the dependence of the surface dust density profile on the extension parameter α . For this figure, the threshold halo mass is fixed to be $2 \times 10^{12} h^{-1} M_\odot$. We compare three cases; $\alpha = 0.1, 1$ and 10 . The dotted lines show the one-halo term. Clearly the extension parameter α affects significantly the amplitude and the shape of the one-halo term. The central surface density is larger for smaller α . This can be easily understood by noting the total dust mass associated with a halo is given by equation (12). On the other hand, α does not affect much the two-halo term at

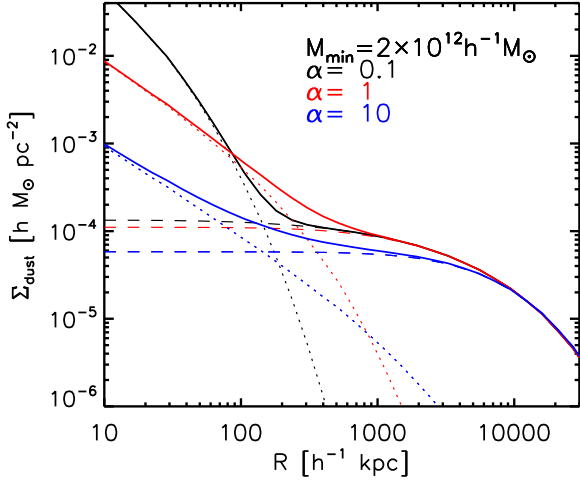


Figure 3. The surface dust density profile as a function of the projected radius for $\alpha = 0.1, 1$ and 10 . The projected radius is the physical distance at $z = 0.36$. The constant model for dust-halo mass ratio is adopted. The dotted and the dashed lines represent the one-halo and the two-halo terms, respectively. The solid lines show the sum of the two terms.

$R \gtrsim 1\text{Mpc}$. The amplitude of the two-halo term is essentially set by the halo bias $b(M_h)$ (see equation [5]).

3 RESULTS

We fit our dust distribution model to the observed surface dust density through least chi-squared minimization. We have two physical parameters, M_{\min} and α , in our model. We have found that poor constraints are obtained on the parameters when both of them are treated as free parameters. Because M_{\min} is already estimated to be $2 \times 10^{12} h^{-1} M_{\odot}$ in Masaki, Fukugita & Yoshida (2012) through detailed comparison of the observed matter distribution with the results of N -body simulations, it is sensible to fit our dust distribution model by treating only α as a free parameter. Namely, the characteristic halo mass can be determined by the gravitational lensing measurement of the matter distribution, whereas the dust distribution extension can be inferred from the observed dust profile.

We evaluate the likelihood of the specific model by the χ^2 value of the model fit to the observed quantities. The obtained best-fit α for the constant and the mass dependent models are, respectively,

$$\alpha = 1.16_{-0.155}^{+0.203} (1\sigma) \text{ for constant model,} \quad (16)$$

$$\alpha = 2.88_{-0.355}^{+0.450} (1\sigma) \text{ for mass dependent model.} \quad (17)$$

Fig. 4 shows the best-fit dust profile of the constant model with $\alpha = 1.16$ and that of the mass dependent model with $\alpha = 2.88$. The data points are from MSFR. Both models for Γ reproduce the observed profile fairly well. It is interesting to compare these two equally good models. The mass dependent model requires a larger α , which is owing to the difference in the typical value of Γ for the two models. At $M_h > 10^{11} h^{-1} M_{\odot}$, Γ of mass dependent model is higher than that of constant model. Because the

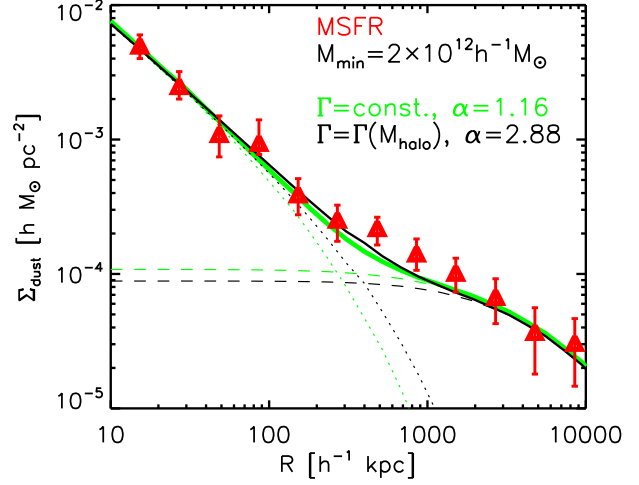


Figure 4. The mean surface dust density profile as a function of the physical projected distance from the center of galaxies at $z = 0.36$. The results from our constant model and mass dependent model are shown by the green and the black lines, respectively. The dotted, the dashed and the solid lines are the one-halo, the two-halo and the total, respectively.

one-halo term is largely contributed by halos with masses $\sim M_{\min} = 2 \times 10^{12} h^{-1} M_{\odot}$, the best fit α is larger for the mass dependent model to match the observed inner dust surface density profile (see Fig.3).

Overall, our simple models reproduce the observed dust profile very well. Intriguingly, both our models suggest $\alpha \sim \mathcal{O}(1)$, i.e., halo dust is distributed over a few hundred kilo parsecs from the galaxies. It is also important that the observed power law surface density $\Sigma_d \propto R^{-0.8}$ at $R = 10\text{kpc} - 10\text{Mpc}$ can be explained with $\alpha \sim \mathcal{O}(1)$. The apparent large-scale dust distribution is explained by the two-halo contributions. Dust is distributed to/over $\sim R_{\text{vir}}$ from a galaxy, but not necessarily up to 10 Mpc as one might naively expect from the observed dust profile.

It is worth discussing the total dust budget in the universe. The amplitude of the two-halo term depends largely on the mean cosmic density of intergalactic dust, $\bar{\rho}_d$ in equation (7)¹. The excellent agreement at large separation between the observed dust density profile and our model prediction shown in Fig. 4 implies that $\Omega_{\text{galaxy dust}}$ should be $\sim 10^{-6}$. Clearly, a significant amount of dust exists around the galaxies. Such “halo dust” can close the cosmic dust budget as discussed more quantitatively by Fukugita (2011).

The intergalactic dust could cause non-negligible extinction and thus could compromise cosmological studies with distant supernovae (Ménard, Kilbinger & Scranton 2010b). We calculate the mean extinction by the intergalactic dust following Zu et al. (2011) (see their equation [2]). With our model mean cosmic density of $\Omega_{\text{galaxy dust}} = 4.7 \times 10^{-6}$, the predicted mean extinction is $\langle A_V \rangle = 0.0090 \text{ mag}$ to $z = 0.5$. Such an opacity is not completely

¹ The halo bias $b(M_h)$ is also a critical factor. However, the characteristic halo mass, and hence $b(M_h)$, is well constrained from the observed matter density profile, as shown in Masaki, Fukugita & Yoshida (2012)

negligible even in the current SNe surveys, and will become important for future surveys that are aimed at determining cosmological parameters with sub-percent precision (Ménard, Kilbinger & Scranton 2010b).

4 DISCUSSION

We have shown that our halo model can reproduce the dust profile around galaxies measured by MSFR. By fitting the model to the observed dust profile, we infer that dust is distributed beyond the virial radius of a galaxy. Several authors proposed radiation-driven transport of dust from galactic discs into intergalactic medium at high redshifts (Aguirre et al. 2001; Bianchi & Ferrara 2005). Zu et al. (2011) showed that galactic winds can disperse dust into the inter-galactic medium efficiently. Such studies generally suggest that dust can travel up to a few $\times 100$ kpc from galaxies if the ejection velocity is $\simeq 100 \text{ km s}^{-1}$. The relatively larger extent radius of dust for our mass dependent model requires very efficient transport mechanisms. Note also that the dust must survive on its way through the galactic halos. Dust in a large, group-size halo could be destroyed by thermal sputtering in hot gas (Bianchi & Ferrara 2005; McGee & Balogh 2010). Clearly, detailed theoretical studies on dust transport are needed.

Fluctuations of the cosmic infrared background (CIB) provide insight into dust distribution around galaxies (e.g., Viero et al. 2009; Amblard et al. 2011). Viero et al. (2009) used BLAST data to measure the CIB power spectrum. Using a halo approach, they found that the observed power spectrum at small angular scales is reproduced if halo dust extends up to a few times of the virial radius of galactic halos. It is remarkably consistent with our conclusion in this Letter. Amblard et al. (2011) compared their measurements of the CIB anisotropies from Herschel wide-area surveys with Viero et al. (2009). Two power spectra are consistent with each other at small scales. Our dust distribution model may provide a key element for studies on the CIB.

Although our model reproduces the observed dust profiles very well, a few improvements can be certainly made. The dust extension α and the dust-halo mass ratio Γ are likely to depend on the halo mass and galaxy type etc (McGee & Balogh 2010). One may need to consider the distribution of satellite galaxies within a halo by using, for example, the halo occupation distribution (HOD). Indeed, we see slight discrepancies between the model predictions and the observation in the dust profiles at $\sim 1 \text{ Mpc}$ (Fig. 4), where the contribution from satellite galaxies are non-negligible (for more detailed modeling, see e.g., Leauthaud et al. 2012). In principle, the HOD parameters can be inferred from the lensing magnification measurement presented by MSFR. However, in order to derive the parameters accurately, one needs to use additional information from observations of the galaxy-galaxy correlation function (Leauthaud et al. 2012). Including these effect in our model is beyond the scope of this Letter, but will be needed in order to interpret data from future wide-field galaxy surveys.

ACKNOWLEDGMENTS

We thank R.S. Asano, M. Fukugita, A. Leauthaud, B. Ménard and T.T. Takeuchi for helpful discussions. SM is supported by the JSPS Research Fellowship. NY acknowledges financial support by the Grant-in-Aid for Young Scientists (S 20674003) by JSPS. The work is supported in part by KMI and GCOE at Nagoya University, by WPI Initiative by MEXT, and by Grant-in-Aid for Scientific Research on Priority Areas No. 467.

REFERENCES

- Aguirre A., Hernquist L., Katz N., Gardner J., Weinberg D., 2001, *ApJ*, 556, L11
- Amblard A., et al., 2011, *Natur*, 470, 510
- Bartelmann M., Schneider P., 2001, *PhR*, 340, 291
- Behroozi P. S., Conroy C., Wechsler R. H., 2010, *ApJ*, 717, 379
- Bianchi S., Ferrara A., 2005, *MNRAS*, 358, 379
- Bryan, G. L., & Norman, M. L. 1998, *ApJ*, 495, 80
- Chelouche D., Koester B. P., Bowen D. V., 2007, *ApJ*, 671, L97
- Cooray, A., & Sheth, R. 2002, *PhR*, 372, 1
- Fukugita, M. 2011, *arXiv:1103.4191*
- Hayashi E., White S. D. M., 2008, *MNRAS*, 388, 2
- Inoue A. K., Kamaya H., 2003, *MNRAS*, 341, L7
- Komatsu, E., Smith, K. M., Dunkley, J., et al. 2011, *ApJs*, 192, 18
- Leauthaud, A., Tinker, J., Bundy, K., et al. 2012, *ApJ*, 744, 159
- Lewis A., Challinor A., Lasenby A., 2000, *ApJ*, 538, 473
- Mandelbaum R., Seljak U., Cool R. J., Blanton M., Hirata C. M., Brinkmann J., 2006, *MNRAS*, 372, 758
- Masaki, S., Fukugita, M., & Yoshida, N. 2012, *ApJ*, 746, 38
- McGee S. L., Balogh M. L., 2010, *MNRAS*, 405, 2069
- Ménard, B., Scranton, R., Fukugita, M., & Richards, G. 2010a, *MNRAS*, 405, 1025 (MSFR)
- Ménard, B., Kilbinger, M., Scranton, R. 2010b, *MNRAS*, 406, 1815
- Navarro, J. F., Frenk, C. S., & White, S. D. M. 1997, *ApJ*, 490, 493
- Seljak, U. 2000, *MNRAS*, 318, 203
- Sheldon E. S., et al., 2004, *AJ*, 127, 2544
- Sheth, R. K., & Tormen, G. 1999, *MNRAS*, 308, 119
- Takeuchi T. T., Buat V., Heinis S., Giovannoli E., Yuan F.-T., Iglesias-Páramo J., Murata K. L., Burgarella D., 2010, *A&A*, 514, A4
- Viero M. P., et al., 2009, *ApJ*, 707, 1766
- York D. G., et al., 2000, *AJ*, 120, 1579
- Zu Y., Weinberg D. H., Davé R., Fardal M., Katz N., Kereš D., Oppenheimer B. D., 2011, *MNRAS*, 412, 1059

This paper has been typeset from a \LaTeX file prepared by the author.